Aberystwyth University

Structural and functional connectivity of the whole brain and subnetworks in individuals with mild traumatic brain injury
Huang, Sihong; Han, Jungong; Zheng, Hairong; Li, Mengjun; Huang, Chuxin; Kui, Xiaoyan; Liu, Jun

Structural and functional connectivity of the whole brain and subnetworks in individuals with mild traumatic brain injury: predictors of patient prognosis

Sihong Huang[1], Jungong Han[2], Hairong Zheng[3], Mengjun Li[1], Chuxin Huang[1], Xiaoyan Kui[4], Jun Liu[1, 5, 6, *]

From the Contents

Graphical Abstract

Subtle abnormalities in structural connectivity during the acute stage, with subsequent recovery trends in both structural and functional connectivity from the acute to chronic stages after mTBI
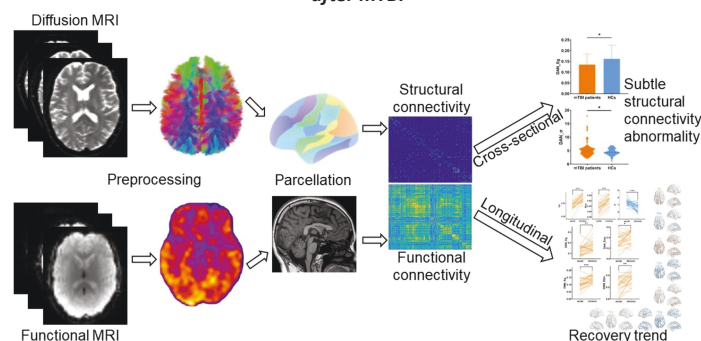
Abstract

Patients with mild traumatic brain injury have a diverse clinical presentation, and the underlying pathophysiology remains poorly understood. Magnetic resonance imaging is a non-invasive technique that has been widely utilized to investigate neurobiological markers after mild traumatic brain injury. This approach has emerged as a promising tool for investigating the pathogenesis of mild traumatic brain injury. Graph theory is a quantitative method of analyzing complex networks that has been widely used to study changes in brain structure and function. However, most previous mild traumatic brain injury studies using graph theory have focused on specific populations, with limited exploration of simultaneous abnormalities in structural and functional connectivity. Given that mild traumatic brain injury is the most common type of traumatic brain injury encountered in clinical practice, further investigation of the patient characteristics and evolution of structural and functional connectivity is critical. In the present study, we explored whether abnormal structural and functional connectivity in the acute phase could serve as indicators of longitudinal changes in imaging data and cognitive function in patients with mild traumatic brain injury. In this longitudinal study, we enrolled 46 patients with mild traumatic brain injury who were assessed within 2 weeks of injury, as well as 36 healthy controls. Resting-state functional magnetic resonance imaging and diffusion-weighted imaging data were acquired for graph theoretical network analysis. In the acute phase, patients with mild traumatic brain injury demonstrated reduced structural connectivity in the dorsal attention network. More than 3 months of follow-up data revealed signs of recovery in structural and functional connectivity, as well as cognitive function, in 22 out of the 46 patients. Furthermore, better cognitive function was associated with more efficient networks. Finally, our data indicated that small-worldness in the acute stage could serve as a predictor of longitudinal changes in connectivity in patients with mild traumatic brain injury. These findings highlight the importance of integrating structural and functional connectivity in understanding the occurrence and evolution of mild traumatic brain injury. Additionally, exploratory analysis based on subnetworks could serve a predictive function in the prognosis of patients with mild traumatic brain injury.

Key Words: cognitive function; cross-section; follow-up; functional connectivity; graph theory; longitudinal study; mild traumatic brain injury; prediction; small-worldness; structural connectivity; subnetworks; whole brain network

Introduction

Mild traumatic brain injury (mTBI) can lead to post-concussion symptoms (Taylor et al., 2017; Center for Disease Control and Prevention, 2023) that include physical, cognitive, and emotional changes (Røe et al., 2009; Meares et al., 2011). The relatively high prevalence of this condition represents a significant burden on society. Although studies have indicated that the structural and functional abnormalities caused by mTBI contribute to these symptoms (Lunkova et al., 2021; Huang et al., 2022; Jang and Seo, 2022; Li et al., 2022a, b, Reddi et al., 2022), the specific mechanisms underlying their persistence remain poorly understood. Therefore, the non-invasive detection

of neurological biomarkers following mTBI has been a major research focus.

Graph theory is a quantitative method of analyzing complex networks. It was extensively employed in several neuroimaging studies to investigate brain structural and functional systems (Bullmore and Sporns, 2009; Imms et al., 2019). Furthermore, the integration of graph theory with machine learning has led to highly accurate classification, highlighting the potential of graph theory in identifying diagnostic biomarkers of mTBI (Fagerholm et al., 2015). However, some previous studies focused on specific populations (e.g., military personnel), and thus may not be generalizable to the general population of mTBI patients encountered in clinical practice (Pandit et al., 2013; Akiki et

[1]Department of Radiology, The Second Xiangya Hospital, Central South University, Changsha, Hunan Province, China; [2]Department of Computer Science, Aberystwyth University, Aberystwyth, Ceredigion, UK; [3]Shenzhen Institutes of Advanced Technology, Chinese Academy of Sciences, Shenzhen, Guangdong Province, China; [4]School of Computer Science and Engineering, Central South University, Changsha, Hunan Province, China; [5]Department of Radiology, Quality Control Center of Hunan Province, Changsha, Hunan Province, China; [6]Clinical Research Center for Medical Imaging of Hunan Province, Changsha, Hunan Province, China

*****Correspondence to:** Jun Liu, MD, junliu123@csu.edu.cn.

https://orcid.org/0000-0002-7851-6782 (Jun Liu)

al., 2018). Additionally, few studies have examined structural connectivity and functional connectivity (FC) in the same patients. Multimodal imaging approaches can capture the heterogeneous nature of mTBI (Lunkova et al., 2021). Accordingly, we explored both structural and functional alterations within the same group of mTBI patients, with the goal of examining their correlation with prognosis. We anticipated that this would supplement our understanding of the development of mTBI.

Cognitive dysfunction is a prominent post-concussion symptom that is associated with various brain subnetworks (e.g. the dorsal attention network (DAN), ventral attention network (VAN), and default mode network (DMN)). The DAN and VAN are task-positive networks responsible for visuospatial attention, detecting stimuli related to sustained attention, and detecting unexpected and unattended stimuli (Amgalan et al., 2022). In contrast, the DMN is a task-negative network composed of densely interconnected white matter tracts. The DMN interacts with task-positive networks and plays a crucial role in cognitive function (Sharp et al., 2011). Prior studies have highlighted the importance of these subnetworks in cognitive function (Franzmeier et al., 2017; Richard et al., 2018; Campbell et al., 2020; Amgalan et al., 2022). We investigated these cognitive networks, in addition to the whole brain networks, to gain a better understanding of the alterations in brain subnetworks following mTBI.

We specifically tested the following hypotheses: (1) mTBI is linked to atypical structural connectivity and FC in the acute stage, which gradually improve throughout the follow-up period. In addition, the change of FC is supported by the change of structural connection; (2) mTBI patients exhibit deficits in cognitive function in the acute phase, which gradually recover over time; and (3) abnormal structural connectivity and FC in mTBI patients are related to impairments in cognitive function. Additionally, we assessed whether abnormal graph metrics observed in the acute phase were correlated with longitudinal changes in cognitive function and network connectivity, as this reflects the predictive ability of these metrics in the acute stage.

Methods

Participants
In this cross-sectional study, a total of 48 mTBI patients were recruited from the emergency department of Second Xiangya Hospital, Central South University, between June 2019 and June 2021. We conducted cross-sectional comparisons with healthy controls (HCs) as well as longitudinal comparisons. The subjects were enrolled after obtaining approval from the Ethics Committee of Second Xiangya Hospital, Central South University (approval No. 086) on February 9, 2019. All participants provided written informed consent. All protocols were executed in accordance with the Ethical Principles for Medical Research Involving Human Subjects in the *Declaration of Helsinki*. This study followed the STrengthening the Reporting of OBservational Studies in Epidemiology (STROBE) guidelines (von Elm et al., 2007).

The inclusion criteria for the mTBI patients were based on the guidelines provided by the World Health Organization Collaborating Center for Neurotrauma Task Force, and the specific inclusion and exclusion criteria are detailed in our previous article (Huang et al., 2022). Patients meeting the following requirements were included: (1) a Glasgow Coma Scale score of 13–15; (2) presence of any of the following: (a) confusion or disorientation, (b) loss of consciousness ≤ 30 minutes, (c) posttraumatic amnesia < 24 hours, (d) transient neurological abnormalities (focal signs or seizure), or (e) intracranial lesion not requiring surgery; and (3) evaluation within 14 days after the onset of mTBI. The exclusion criteria were: (1) age below 18 or above 60 years; (2) presence of severe psychiatric disease, severe somatic disease, or drug abuse; (3) history of complicated mild, moderate, or severe traumatic brain injury (TBI) or other diseases associated with brain pathology; (4) structural abnormality; and (5) contraindications for magnetic resonance imaging (MRI). A total of 38 HCs were recruited through various social platforms, such as QQ and WeChat, at the same time as the mTBI patient recruitment. The exclusion criteria for the HCs matched that of the mTBI patients.

All subjects underwent comprehensive clinical and psychiatric evaluations via face-to-face interviews conducted by trained staff members. The evaluations encompassed various clinical characteristics, such as injury time, post-injury symptoms, the interval between the injury and MRI scan, and follow-up assessments. The detailed demographic characteristics can be found in **Tables 1** and **2**.

MRI acquisition
MRI data were acquired using a 3T MRI scanner (MAGNETOM Skyra, Siemens Healthcare, Erlangen, Germany) equipped with a 32-channel head coil. Clinical diagnostic sequences, high-resolution structural MRI sequences, and susceptibility-weighted imaging were used to thoroughly assess and rule out any structural abnormalities. Two experienced neuroradiologists with over 10 years of neuroimaging expertise evaluated the images. In cases of disagreement between the two observers, a consensus was reached through discussion. Resting state functional MRI data were acquired with a repetition time/echo time of 2000/30 ms, thickness of 4.0 mm with no gap, field of view of 240 × 240 mm², flip angle of 90°, matrix size of 64 × 64, and 36 slices. The acquisition time for resting state functional MRI was 6 minutes and 6 seconds, and the participants were instructed to relax, close their eyes, and avoid falling asleep. We previously gave the detailed scan parameters for diffusion MRI (Huang et al., 2022). The participants underwent scanning in a supine position with foam padding placed between their head and the head coil to minimize head motion.

Table 1 │ Demographic and clinical characteristics of mTBI patients and HCs

	mTBI	HCs	t/Z/χ²	P
Number	46	36		
Sex (male/female)	19/27	17/19	0.287	0.59[a]
Age (yr)	37.07±9.94	40.92±8.54	−1.85	0.068[b]
Education (yr)	12 (9–16)	15 (11.25–16)	−1.14	0.25[c]
Cause of injury				
Vehicle accident	15			
Assault	15			
Fall	9			
Other	7			
Injury and MRI scan interval (h)	48.50 (26.50–93.25)			
Neuropsychological tests				
TMT-A	46.52 (31.07–60.06)	45.68 (39.48–58.26)	−0.46	0.65[c]
TMT-B	97.10 (75.32–187)	100.92 (70.78–122)	−0.61	0.54[c]
DSST	53 (36.5–60)	55 (46.75–64.25)	−1.08	0.28[c]

DSST: Digital Symbol Substitution Test; HCs: healthy controls; MRI: magnetic resonance imaging; mTBI: mild traumatic brain injury; TMT: Trail Making Test. Data were analyzed by chi-square test[a], unpaired two-sample *t*-test[b] or Kruskal-Wallis test[c]. The distributed data are expressed as mean ± standard deviation, and the non-normal distributed data are expressed as median and quartiles.

Table 2 │ Demographic and clinical characteristics of mTBI patients in the acute and chronic stage

	Acute stage	Chronic stage	t/Z/χ²	P
Number		22		
Sex (n, female)		15		
Age (yr)		37.38±11.68		
Education (yr)		15 (9–16)		
Cause of injury (n)				
Vehicle accident		4		
Assault		9		
Fall		5		
Other		4		
Neuropsychological tests				
TMT-A	54.04±23.67	43.95±19.90	2.24	0.037
TMT-B	110.24±47.59	96.39±45.48	1.1	0.29
DSST	48.76±17.96	55.14±18.36	−1.22	0.24

DSST: Digital Symbol Substitution Test; HCs: healthy controls; mTBI: mild traumatic brain injury; TMT: Trail Making Test. Data in neuropsychological tests were analyzed by paired two-sample *t*-test. The distributed data are expressed as mean ± standard deviation, and the non-normal distributed data are expressed as median and quartiles.

Neuropsychological testing
All participants completed the Digit Symbol Substitution Test (DSST) and Trail Making Tests (TMT) A and B, as described in our previous work (Huang et al., 2022). The DSST is commonly used to assess processing speed, sustained attention, and working memory (Wechsler, 1997; Qin et al., 2017). In these tests, the accuracy of the written symbols and the speed of completion reflect the level of cognition. The TMT-A is administered as a baseline measure of motor and visual search speed (Sánchez-Cubillo et al., 2009; Misdraji and Gass, 2010), while the TMT-B (Horton and Hartlage, 1994) is widely used as a measure of set shifting and inhibition (Arbuthnott and Frank, 2000; MacPherson et al., 2017). These tests are well-established tools used in neuropsychological assessments, and provide insight into cognitive processing speed and executive functioning (Asken et al., 2018). The neuropsychological tests were administered on the same day as the MRI.

Functional image preprocessing and network construction
We utilized a GRaph thEoreTical Network Analysis (GRETNA) (www.nitrc.org) for standard data preprocessing (Wang et al., 2015). The initial 10 volumes for each subject were discarded to allow for magnetization equilibration, and the remaining 170 volumes were subjected to slice-time correction and three-dimensional head motion correction. Subjects exhibiting a maximum displacement over 2 mm or head rotation exceeding 2° were excluded from the analysis. The high-resolution structural images were co-registered to the mean of the realigned echo planar images on an individual basis. The transformed structural images were then segmented into gray matter, white matter, and cerebrospinal fluid. We employed DARTEL (Ashburner, 2007) to compute transformations from individual native space to Montreal Neurological Institute (MNI) space, and the resulting images were resampled to a voxel size of 3 × 3 × 3 mm³. Subsequently, a 4-mm FWHM Gaussian kernel was applied to smooth the images. Nuisance covariates, including the white matter signal, cerebrospinal fluid signal, global signal, and Friston 24-parameter head motion parameters were regressed from the time series of all voxels to mitigate the impact of confounding factors. Finally, a temporal bandpass filter (0.01–0.08 Hz) was employed to reduce low-frequency

drift, physiological high-frequency noise, and cardiac noise. We used the Brainnetome Atlas (Fan et al., 2016) to define graph nodes, and divided the brain into 246 cortical and subcortical regions of interest (ROI). We extracted the average time series of all voxels within each ROI to derive a representative time series for each subject. We then calculated Pearson's correlation coefficients for the mean time series of the 246 ROIs to obtain a 246 × 246 connection matrix (FC matrix).

Structural image preprocessing and network construction

Before preprocessing, we performed a visual inspection of the diffusion images for each subject to ensure the absence of significant artifacts, such as those resulting from head motion. We used Pipeline for Analyzing braiN Diffusion imAges (PANDA) (www.nitrc.org) to carry out whole-brain fiber deterministic tractography and generate a connectivity matrix for each participant based on the preprocessed diffusion images (Cui et al., 2013). We used the Fiber Assignment by Continuous Tracking algorithm (Mori et al., 1999) to compute the white matter fiber tracts throughout the entire brain. Additionally, we used the Brainnetome template to define the 246 nodes, and calculated the fiber number (FN) and fractional anisotropy (FA) of the fibers connecting each pair of ROIs to define the edges in the connectivity matrix.

Graph theoretical network analysis

We used GRETNA to calculate the graph metrics of the FC, FA, and FN networks. The sparsity was calculated by dividing the total number of edges by the maximum number of possible edges. Given the dense and highly variable properties of functional networks and the sparse and stable properties of structural networks, we only calculated the threshold for the sparsity of the functional networks (Imms et al., 2019). The sparsity of the functional networks ranged from 0.05 to 0.35, with intervals of 0.05. The minimum sparsity was set to ensure that there were no isolated nodes in the network. The maximum sparsity was set to ensure that the small-world index was larger than 1.1 for all healthy subjects. We estimated the global and local efficiency (Eg and Eloc), clustering coefficient (Cp), and small-world index (σ) to investigate the global network properties. We estimated the nodal efficiency (Ne), nodal local efficiency (NLe), nodal clustering coefficient (NCp), nodal shortest path length (NLp), betweenness centrality (Bc), and degree centrality (Dc) to investigate the regional (nodal) properties. The details of these graph metrics are shown in **Table 3**. To address the issue of multiple comparisons, we employed a correction method for family-wise error. This was based on the 246 × 246 connection matrix and the network partition used by Yeo et al. (2011). We extracted the subnetwork connection matrix of the DMN, VAN, and DAN for the above graph theoretical network analysis. We used BrainNet Viewer (www.nitrc.org) to visualize the brain connectivity data (Xia et al., 2013).

Table 3 | Summary of global and nodal graph theory metrics

	Metric	Abbreviation	Definition
Global metrics	Global efficiency	Eg	Average degree of information transfer among network nodes; the average inverse shortest path length.
	Local efficiency	Eloc	Average degree of information transfer between each node in the network and its neighboring nodes.
	Clustering coefficient	Cp	Averaged proportion of each node's neighbors that are also considered to be neighbors.
	Small-worldness	σ	Ratio of clustering coefficient to path length, both of which are standardized measures within the network.
Nodal metrics	Nodal efficiency	Ne	Efficiency of information transfer from a specific node to all other nodes in the network.
	Nodal local efficiency	NLe	Efficiency of information transfer from a specific node to its nearby or neighboring nodes.
	Nodal Clustering coefficient	NCp	Proportion of a given node's neighbors that are also connected to each other.
	Nodal Shortest path length	NLp	Minimum number of edges among a given node and all other nodes in the graph.
	Betweenness centrality	Bc	Frequency that a specific node is part of shortest paths to all other (whole) network nodes.
	Degree centrality	Dc	Total edge count for a specific node.

Statistical analysis

The demographic characteristics and neuropsychological data were analyzed using IBM SPSS Statistics for Windows (Version 24.0, IBM Corp., Armonk, NY, USA). Statistical tests such as unpaired two-sample *t*-tests, chi-square tests, Kruskal-Wallis tests, paired two-sample *t*-tests, and Wilcoxon tests were conducted to assess differences in age, gender, education, and neuropsychological test scores among groups. To examine the relationship between graph metrics and neuropsychological test scores, we performed

partial correlation analyses after controlling for sex, age, and education. Additionally, we used partial correlation analyses to explore the associations between graph metrics in the acute stage and longitudinal changes in graph metrics, as well as between graph metrics in the acute stage and longitudinal changes in cognitive performance, with the number of follow-up days as a covariate. Pearson's and Spearman's correlations were calculated to examine the associations between graph metrics and cognitive scores, as well as between longitudinal changes in graph metrics and longitudinal changes in cognitive scores, specifically within the mTBI group. To account for multiple comparisons, correlations were adjusted using family-wise error correction.

Results

Demographic and clinical characteristics

Table 1 provides an overview of the characteristics of the mTBI patients and HCs. Two patients and two HCs were excluded because of major image artifacts. The sample included 46 mTBI patients (mean age, 37.07 years; 19 men) and 36 HCs (mean age, 40.92 years; 17 men). There were no significant differences in sex, age, or education between the patients and HCs. The median time interval between injury and the MRI scan was 48.5 hours. The detailed characteristics of the mTBI patients during the acute stage and follow up period (chronic phase) are provided in **Table 2**. Twenty-two patients (mean age, 37.38 years; seven men) completed two MRI scans. The median follow-up period was 124 days. The flowchart of our study is presented in **Figure 1**.
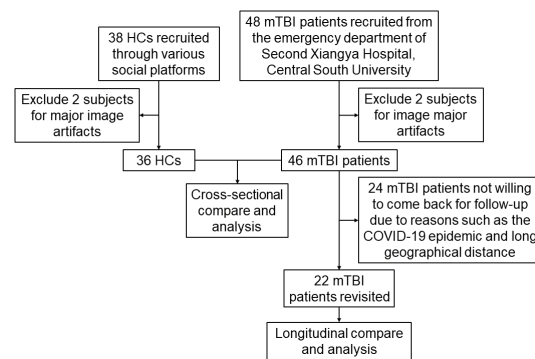

Figure 1 | The flowchart for this study.
COVID-19: Corona Virus Disease 2019; HC: healthy control; mTBI: mild traumatic brain injury.

Neuropsychological test results

Data from five mTBI patients were missing because of hand fractures (three patients) and the need to maintain a reclined position (two patients). When compared with the HCs, the mTBI patients exhibited a tendency towards declined cognitive function, but the differences were not statistically significant (**Table 1**). However, cognitive function, as reflected by TMT-A, demonstrated a significant improvement during the follow-up period (**Table 2**).

Global graph theoretical results

The cross-sectional analysis revealed no significant differences in FN or FC between the mTBI patients and HCs. However, we observed differences in FA connectivity between the patient groups. In terms of the DAN, the mTBI patients exhibited a significantly lower Eg compared with the HCs ($t = -2.18$, $P = 0.032$). Additionally, the σ within the DAN was found to be significantly higher in mTBI patients compared with the HCs ($t = 2.01$, $P = 0.048$; **Figure 2**).

The longitudinal analysis revealed significant changes in graph metrics between the first and second MRI scans (acute and chronic stages). At the whole brain level, Eg (FA: $t = -8.93$, $P < 0.001$; FN: $t = -13.043$, $P < 0.001$; FC: $t = -5.32$, $P < 0.001$) and Eloc (FA: $t = -8.50$, $P < 0.001$; FN: $t = -7.88$, $P < 0.001$) were significantly increased, while σ was significantly decreased (FA: $t = 4.78$, $P < 0.001$; FN: $t = 3.43$, $P = 0.0025$; FC: $t = 5.61$, $P < 0.001$). In the DAN and DMN, both global and local efficiency were significantly increased after more than 3 months of follow-up (FA: DAN: Eg: $t = -3.61$, $P = 0.0016$; Eloc: $t = -2.49$, $P = 0.021$; DMN: Eg: $t = -5.09$, $P < 0.001$; Eloc: $t = -3.40$, $P = 0.0027$; FN: DAN: Eg: $t = -5.19$, $P < 0.001$; Eloc: $t = -2.84$, $P = 0.0097$; DMN: Eg: $t = -7.48$, $P < 0.001$; Eloc: $t = -5.16$, $P < 0.001$; FC: DAN: Eg: $t = -2.85$, $P = 0.010$; Eloc: $t = -2.44$, $P = 0.024$ DMN: $t = -3.15$, $P = 0.028$). Additionally, in the FC network, the σ of the DAN ($t = -2.18$, $P = 0.041$) and the Eg of the VAN ($t = -2.95$, $P = 0.0080$) showed a significant increase over the follow-up period. The results are presented in **Figures 3–5**.

The nodal graph theoretical results showed no significant differences between the mTBI patients and HCs. However, in the chronic stage, the patients showed higher Dc, Ne, and NLe, shorter NLp, and lower NCp in the superior frontal gyrus (SFG), middle frontal gyrus (MFG), precentral gyrus (PrG), superior temporal gyrus (STG), middle temporal gyrus (MTG), inferior temporal gyrus (ITG), superior parietal lobule (SPL), inferior parietal lobule (IPL), precuneus, postcentral gyrus (PoG), cingulate gyrus (CG), medioventral occipital cortex (MVOcC), lateral occipital cortex (LOoC), hippocampus, basal ganglia (BG), and thalamus. These results indicate that the network connections were more efficient in the chronic versus acute stage (**Figure 6**).
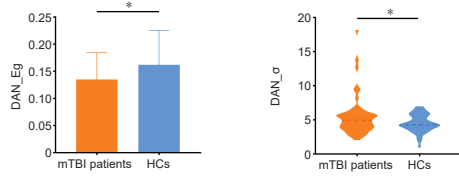
Figure 2 | Cross-sectional results of structural brain connectivity networks (edges defined by FA).
The mTBI patients showed a lower Eg and a higher σ in the DAN compared with the HCs. *$P < 0.05$ (unpaired two-sample *t*-test for Eg and Kruskal-Wallis test for σ). DAN: Dorsal attention network; Eg: global efficiency; FA: fractional anisotropy; HCs: healthy controls; mTBI: mild traumatic brain injury; σ: small-worldness.
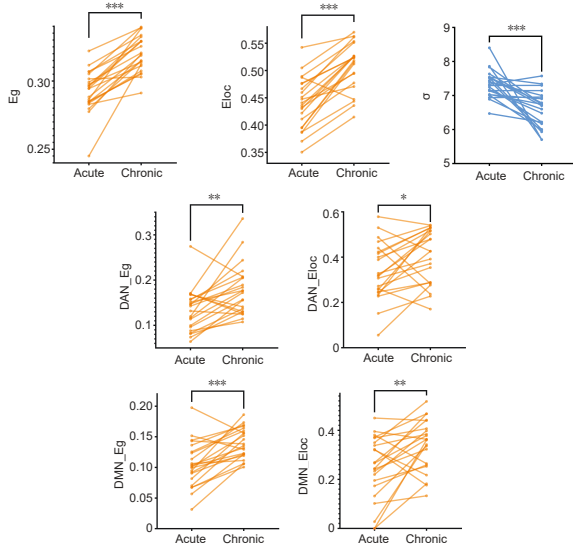

Figure 3 | Longitudinal changes in structural brain connectivity networks (edges defined by FA).
During the follow-up period, mTBI patients showed increased Eg and Eloc, and decreased σ at the whole brain level. Eg and Eloc were also increased in the DAN and DMN. *$P < 0.05$, **$P < 0.01$, ***$P < 0.001$. Normally distributed data (Eg, Eloc, σ, DAN_Eg, DMN_Eg, and DMN_Eloc) were analyzed with paired two-sample *t*-tests, and non-normally distributed data (DAN_Eloc) were analyzed with Wilcoxon tests. DAN: Dorsal attention network; DMN: default mode network; Eg: global efficiency; Eloc: local efficiency; FA: fractional anisotropy; mTBI: mild traumatic brain injury; σ: small-worldness.
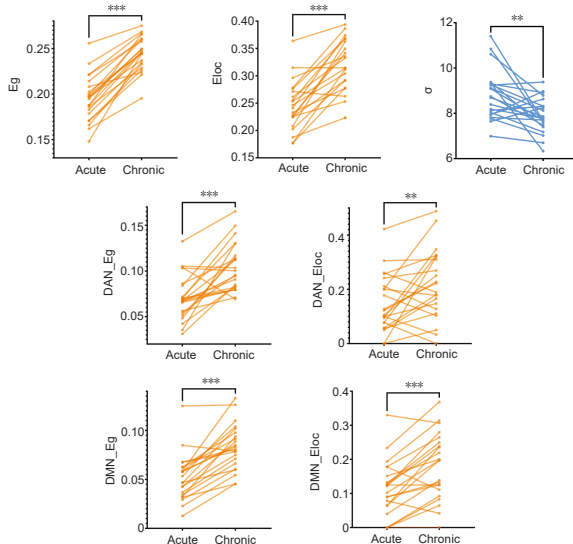

Figure 4 | Longitudinal changes in structural brain connectivity networks (edges defined by FN).
During the follow-up period, mTBI patients showed increased Eg and Eloc, and decreased σ at the whole brain level. Eg and Eloc were also increased in the DAN and DMN. **$P < 0.01$, ***$P < 0.001$ (paired two-sample *t*-tests). DAN: Dorsal attention network; DMN: default mode network; Eg: global efficiency; Eloc: local efficiency; FN: fiber number; mTBI: mild traumatic brain injury; σ: small-worldness.
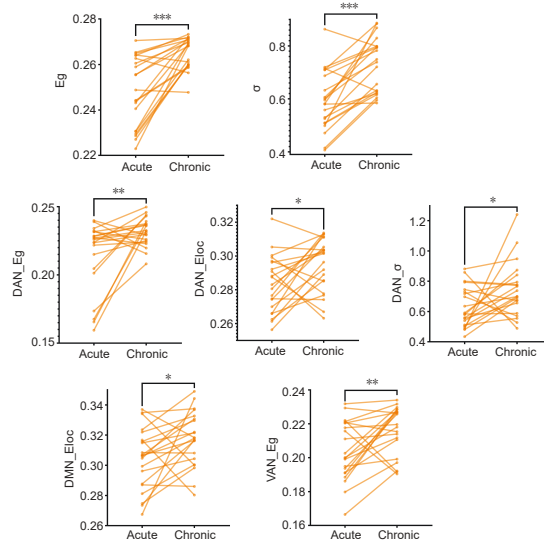

Figure 5 | Longitudinal results of functional brain connectivity networks.
During the follow-up period, mTBI patients showed increased Eg and σ at the whole brain level. In the DAN, we found increased Eg, Eloc, and σ in mTBI patients. We also found increased Eloc in the DMN and increased Eg in the VAN. *$P < 0.05$, **$P < 0.01$, ***$P < 0.001$. Normally distributed data (Eg, σ, DAN_Eloc, DAN_σ, DMN_Eloc, VAN_Eg) were analyzed with paired two-sample *t*-tests, and non-normally distributed data (DAN_Eg) were analyzed with Wilcoxon tests. DAN: Dorsal attention network; DMN: default mode network; Eg: global efficiency; Eloc: local efficiency; mTBI: mild traumatic brain injury; VAN: ventral attention network; σ: small-worldness.
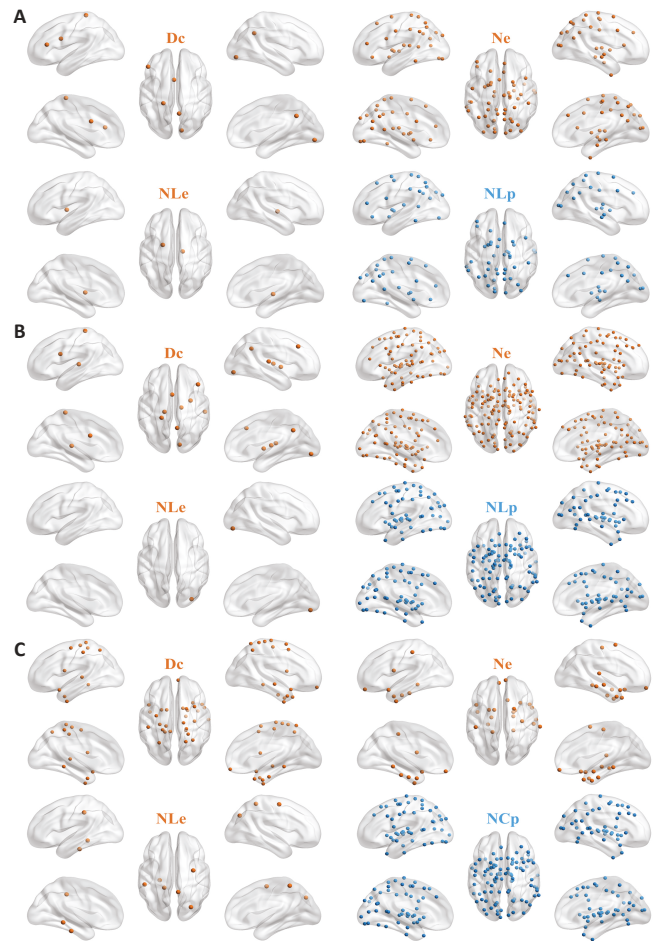

Figure 6 | Longitudinal nodal graph theory metrics in mTBI patients.
(A) Edges defined by FA. (B) Edges defined by FN. (C) Edges defined by FC. Orange color represents increased nodal metrics and blue color represents decreased nodal metrics during the follow-up period. Dc: Degree centrality; FA: fractional anisotropy; FC: functional connectivity; FN: fiber number; mTBI: mild traumatic brain injury; NCp: nodal clustering coefficient; Ne: nodal efficiency; NLe: nodal local efficiency; NLp: nodal shortest path length.

Correlation results

Overall, more efficient networks (higher Dc, Ne, Eloc, and shorter NLp) were associated with better cognition. However, we found no statistically significant differences after family-wise error correction. The correlation between the graph metrics in the acute stage and longitudinal changes in the graph metrics showed various trends. However, after family-wise error correction, we found a significant correlation between the σ of the DAN in the acute stage and the change in nodal efficiency in the right middle temporal gyrus ($r = 0.820$, $P < 0.001$; **Figure 7**).
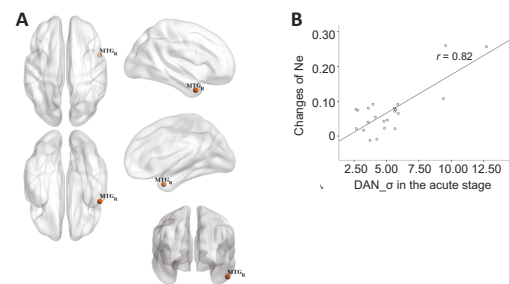

Figure 7 | Partial correlations between the σ of the DAN in the acute stage and changes in Ne.
(A) Node location in the right middle temporal gyrus. (B) The scatter plot showing the partial correlation. Longitudinal changes in Ne were positively correlated with the σ of the DAN in the acute stage and there was a significant correlation in the right middle temporal gyrus. DAN: Dorsal attention network; MTG: middle temporal gyrus; Ne: nodal efficiency; R: right; σ: small-worldness.

Discussion

In the acute stage, the mTBI patients showed structural connectivity deficits in the DAN with the edges weighted according to the FA. However, after more than 3 months of follow-up assessments, we founded a tendency towards recovery in structural connectivity and FC, as well as cognitive function in the patient group. Furthermore, better cognitive function was correlated with more efficient networks. Notably, the small-worldness of the DAN in the acute stage predicted longitudinal changes in connectivity among the mTBI patients.

In the cross-sectional comparison, we found no significant differences in whole brain connectivity, indicating subtle changes in structural connectivity and FC in the acute stage after mTBI. Our findings are in alignment with a growing body of evidence indicating no significant differences in whole brain connectivity between mTBI patients and HCs (van der Horn et al., 2017). Exploratory analysis of subnetworks could be used as an additional method to better understand subtle changes in the acute stage. In the current study, both mTBI patients and HCs exhibited typical features of a small-world system, characterized by a normalized clustering coefficient considerably greater than 1, a normalized characteristic path length close to 1, and small-worldness index significantly above 1. However, within the DAN, the mTBI group demonstrated a significantly higher σ compared with the HCs. Although we observed higher clustering coefficients and characteristic path lengths in the mTBI patients in terms of other small-world indices, these differences did not reach statistical significance. These results are similar to previous findings in children reported by Yuan et al. (2015), suggesting that the network in the mTBI group had more local connections and fewer long-distance connections. The increase in short connections suggest enhanced local robustness and redundancy, while the longer path lengths imply that information traversed a greater number of nodes to reach its ultimate destination (Rubinov and Sporns, 2010). These findings are consistent with those of studies reviewed by a meta-analysis, especially in terms of mTBI patients (Imms et al., 2019). Our findings regarding a decrease in global efficiency also support this point. This pattern may be the initial adaptive response in the acute stage to compensate for the decreased efficiency in integrating the anatomically segregated brain structures. The positive σ correlation in the DAN and the change in Ne from the first to second scan also suggest a possible compensatory mechanism. Similarly, the compensatory trends observed after TBI have been validated by pathological studies conducted at various research institutes (Chao et al., 2019; Capizzi et al., 2020). A higher small-worldness in the acute stage has been associated with better nodal efficiency recovery, indicating that small-worldness is a potential predictor of outcome after mTBI. In contrast, a negative correlation between small-worldness and outcome was reported by Roine et al. (2022) in mTBI patients 8 months after injury. They found that networks exhibiting overly small-world patterns showed reduced efficiency in terms of global integration, leading to poorer outcomes. Another study found higher small-worldness in TBI patients in the chronic stage (Yuan et al., 2017). Those results suggest that chronic impairment is associated with small-worldness, while our results indicate that brain compensation occurs in the acute stage, and that this compensatory capacity reflects patient outcomes.

In our longitudinal comparison, we identified a noticeable trend towards recovery in both the global and nodal characteristics of the structural and functional networks. This trend is consistent with other studies that have reported recovered connectivity (Dall'Acqua et al., 2017). Dall'Acqua et al. (2017) also observed recovery of structural connectivity and FC one year after trauma. This recovery trend has been detected using various methods such as diffusion tensor imaging (Mayer et al., 2010). However, some studies have failed to detect longitudinal changes in connectivity (Mayer et al., 2011), while others reported weakened connectivity within 3 months after injury followed by an increase within 6 months (Bharath et al., 2015). The timing of imaging post mTBI may have significant implications for the variability of results across different studies. Future work should consider recruiting patients at different time points after injury to better understand the recovery process. Additionally, different analysis methods and the heterogeneous nature of mTBI and patient characteristics may also explain the different results observed in various studies. Overall, our findings support previous evidence indicating that functional and structural connectivity are strongly interrelated (Hagmann et al., 2008; Honey et al., 2009; van den Heuvel et al., 2009; Yuan et al., 2015).

During the follow-up period, we found that cognitive function was gradually recovered following the restoration of structural connectivity and FC. These findings are in line with an earlier study (Kuceyeski et al., 2019). Here, we found that greater network efficiency was associated with better cognitive function. This is consistent with similar findings in TBI patients reported by Caeyenberghs et al. (2014), indicating that similar mechanisms may exist across mild to severe TBI. Additionally, we found that longer path length was correlated with lower cognitive performance, which is in agreement with another study (Kim et al., 2014). The above-mentioned findings are further supported by pathological studies that have shown a correlation between TBI-induced abnormalities and cognitive impairments at the cellular and subcellular levels (Liu et al., 2021; Bolte et al., 2023). However, a study by van der Horn et al. (2017) reported the opposite correlation, as in, decreased global efficiency was associated with improved cognitive recovery. This discrepancy could be attributed, at least in part, to the diverse characteristics of individuals with mTBI (e.g., traumatic position, cause of injury). Nonetheless, it is important to note that none of the correlations remained significant after adjusting for multiple comparisons. Therefore, it is appropriate to consider the correlations between the longitudinal graph theoretical results and cognitive function as exploratory in nature.

The current study had several limitations. First, the study had a relatively small sample size, particularly in the longitudinal comparison group. As a result of the COVID-19 pandemic, the number of subjects that could be recruited decreased significantly. Future studies should aim to recruit larger numbers of mTBI patients to increase the statistical power and generalizability of the results. Second, the structural network construction relied on deterministic fiber tracking, which might not fully represent the true anatomical connections. The use of alternative tracking methods, such as probabilistic fiber tracking, should be explored and validated. Third, the presence of concomitant injuries in other body regions might have influenced the performance of mTBI patients, although efforts were made to minimize the inclusion of these patients. Including a trauma control group could help to address this limitation in future studies. Finally, FA and FN lack microstructural specificity when used as measures of structural connectivity. Advanced measures of white matter, such as fiber density and edge weights, should be explored in future research.

In conclusion, mTBI patients exhibit subtle changes in structural connectivity in the acute stage only, which are reflected by subnetwork connectivity. However, both connectivity and cognitive function tended to recover during the follow-up period. Combined analysis of structural connectivity and FC can better reflect the occurrence and evolution of mTBI. Additionally, exploratory analysis based on subnetworks can help to characterize these changes in more detail and may have value as a predictor of prognosis.

Additional file:

Additional file 1: STROBE Statement—checklist of items that should be included in reports of observational studies.

References

Akiki TJ, Averill CL, Wrocklage KM, Scott JC, Averill LA, Schweinsburg B, Alexander-Bloch A, Martini B, Southwick SM, Krystal JH, Abdallah CG (2018) Default mode network abnormalities in posttraumatic stress disorder: A novel network-restricted topology approach. Neuroimage 176:489-498.

Amgalan A, Maher AS, Imms P, Ha MY, Fanelle TA, Irimia A (2022) Functional connectome dynamics after mild traumatic brain injury according to age and sex. Front Aging Neurosci 14:852990.

Arbuthnott K, Frank J (2000) Trail making test, part B as a measure of executive control: validation using a set-switching paradigm. J Clin Exp Neuropsychol 22:518-528.

Ashburner J (2007) A fast diffeomorphic image registration algorithm. Neuroimage 38:95-113.

Asken BM, DeKosky ST, Clugston JR, Jaffee MS, Bauer RM (2018) Diffusion tensor imaging (DTI) findings in adult civilian, military, and sport-related mild traumatic brain injury (mTBI): a systematic critical review. Brain Imaging Behav 12:585-612.

Bharath RD, Munivenkatappa A, Gohel S, Panda R, Saini J, Rajeswaran J, Shukla D, Bhagavatula ID, Biswal BB (2015) Recovery of resting brain connectivity ensuing mild traumatic brain injury. Front Hum Neurosci 9:513.

Bolte AC, Shapiro DA, Dutta AB, Ma WF, Bruch KR, Kovacs MA, Royo Marco A, Ennerfelt HE, Lukens JR (2023) The meningeal transcriptional response to traumatic brain injury and aging. Elife 12:e81154.

Bullmore E, Sporns O (2009) Complex brain networks: graph theoretical analysis of structural and functional systems. Nat Rev Neurosci 10:186-198.

Caeyenberghs K, Leemans A, Leunissen I, Gooijers J, Michiels K, Sunaert S, Swinnen SP (2014) Altered structural networks and executive deficits in traumatic brain injury patients. Brain Struct Funct 219:193-209.

Campbell MC, Jackson JJ, Koller JM, Snyder AZ, Kotzbauer PT, Perlmutter JS (2020) Proteinopathy and longitudinal changes in functional connectivity networks in Parkinson disease. Neurology 94:e718-728.

Capizzi A, Woo J, Verduzco-Gutierrez M (2020) Traumatic brain injury: an overview of epidemiology, pathophysiology, and medical management. Med Clin North Am 104:213-238.

Center for Disease Control and Prevention (2023) Traumatic brain injury and concussion. https://www.cdc.gov/traumaticbraininjury/index.html. Accessed April 20, 2023.

Chao H, Lin C, Zuo Q, Liu Y, Xiao M, Xu X, Li Z, Bao Z, Chen H, You Y, Kochanek PM, Yin H, Liu N, Kagan VE, Bayır H, Ji J (2019) Cardiolipin-dependent mitophagy guides outcome after traumatic brain injury. J Neurosci 39:1930-1943.

Cui Z, Zhong S, Xu P, He Y, Gong G (2013) PANDA: a pipeline toolbox for analyzing brain diffusion images. Front Hum Neurosci 7:42.

Dall'Acqua P, Johannes S, Mica L, Simmen HP, Glaab R, Fandino J, Schwendinger M, Meier C, Ulbrich EJ, Müller A, Baetschmann H, Jäncke L, Hänggi J (2017) Functional and structural network recovery after mild traumatic brain injury: a 1-year longitudinal study. Front Hum Neurosci 11:280.

Fagerholm ED, Hellyer PJ, Scott G, Leech R, Sharp DJ (2015) Disconnection of network hubs and cognitive impairment after traumatic brain injury. Brain 138:1696-1709.

Fan L, Li H, Zhuo J, Zhang Y, Wang J, Chen L, Yang Z, Chu C, Xie S, Laird AR, Fox PT, Eickhoff SB, Yu C, Jiang T (2016) The human brainnetome atlas: a new brain atlas based on connectional architecture. Cereb Cortex 26:3508-3526.

Franzmeier N, Buerger K, Teipel S, Stern Y, Dichgans M, Ewers M (2017) Cognitive reserve moderates the association between functional network anti-correlations and memory in MCI. Neurobiol Aging 50:152-162.

Hagmann P, Cammoun L, Gigandet X, Meuli R, Honey CJ, Wedeen VJ, Sporns O (2008) Mapping the structural core of human cerebral cortex. PLoS Biol 6:e159.

Honey CJ, Sporns O, Cammoun L, Gigandet X, Thiran JP, Meuli R, Hagmann P (2009) Predicting human resting-state functional connectivity from structural connectivity. Proc Natl Acad Sci U S A 106:2035-2040.

Horton AM, Jr., Hartlage LC (1994) The Halstead-Reitan neuropsychology test battery: theory and clinical interpretation second edition. Arch Clin Neuropsychol 9:289-290.

Huang S, Huang C, Li M, Zhang H, Liu J (2022) White matter abnormalities and cognitive deficit after mild traumatic brain injury: comparing DTI, DKI, and NODDI. Front Neurol 13:803066.

Imms P, Clemente A, Cook M, D'Souza W, Wilson PH, Jones DK, Caeyenberghs K (2019) The structural connectome in traumatic brain injury: A meta-analysis of graph metrics. Neurosci Biobehav Rev 99:128-137.

Jang SH, Seo YS (2022) Diffusion tensor tractography characteristics of axonal injury in concussion/mild traumatic brain injury. Neural Regen Res 17:978-982.

Kim J, Parker D, Whyte J, Hart T, Pluta J, Ingalhalikar M, Coslett HB, Verma R (2014) Disrupted structural connectome is associated with both psychometric and real-world neuropsychological impairment in diffuse traumatic brain injury. J Int Neuropsychol Soc 20:887-896.

Kuceyeski AF, Jamison KW, Owen JP, Raj A, Mukherjee P (2019) Longitudinal increases in structural connectome segregation and functional connectome integration are associated with better recovery after mild TBI. Hum Brain Mapp 40:4441-4456.

Li MJ, Huang SH, Huang CX, Liu J (2022a) Morphometric changes in the cortex following acute mild traumatic brain injury. Neural Regen Res 17:587-593.

Li MJ, Yeh FC, Huang SH, Huang CX, Zhang H, Liu J (2022b) Differential tractography and correlation tractography findings on patients with mild traumatic brain injury: a pilot study. Front Hum Neurosci 16:751902.

Liu Q, Bhuiyan MIH, Liu R, Song S, Begum G, Young CB, Foley LM, Chen F, Hitchens TK, Cao G, Chattopadhyay A, He L, Sun D (2021) Attenuating vascular stenosis-induced astrogliosis preserves white matter integrity and cognitive function. J Neuroinflammation 18:187.

Lunkova E, Guberman GI, Ptito A, Saluja RS (2021) Noninvasive magnetic resonance imaging techniques in mild traumatic brain injury research and diagnosis. Hum Brain Mapp 42:5477-5494.

MacPherson SE, Cox SR, Dickie DA, Karama S, Starr JM, Evans AC, Bastin ME, Wardlaw JM, Deary IJ (2017) Processing speed and the relationship between Trail Making Test-B performance, cortical thinning and white matter microstructure in older adults. Cortex 95:92-103.

Mayer AR, Mannell MV, Ling J, Gasparovic C, Yeo RA (2011) Functional connectivity in mild traumatic brain injury. Hum Brain Mapp 32:1825-1835.

Mayer AR, Ling J, Mannell MV, Gasparovic C, Phillips JP, Doezema D, Reichard R, Yeo RA (2010) A prospective diffusion tensor imaging study in mild traumatic brain injury. Neurology 74:643-650.

Meares S, Shores EA, Taylor AJ, Batchelor J, Bryant RA, Baguley IJ, Chapman J, Gurka J, Marosszeky JE (2011) The prospective course of postconcussion syndrome: the role of mild traumatic brain injury. Neuropsychology 25:454-465.

Misdraji EL, Gass CS (2010) The Trail Making Test and its neurobehavioral components. J Clin Exp Neuropsychol 32:159-163.

Mori S, Crain BJ, Chacko VP, van Zijl PC (1999) Three-dimensional tracking of axonal projections in the brain by magnetic resonance imaging. Ann Neurol 45:265-269.

Pandit AS, Expert P, Lambiotte R, Bonnelle V, Leech R, Turkheimer FE, Sharp DJ (2013) Traumatic brain injury impairs small-world topology. Neurology 80:1826-1833.

Qin B, Xun P, Jacobs DR, Jr., Zhu N, Daviglus ML, Reis JP, Steffen LM, Van Horn L, Sidney S, He K (2017) Intake of niacin, folate, vitamin B-6, and vitamin B-12 through young adulthood and cognitive function in midlife: the Coronary Artery Risk Development in Young Adults (CARDIA) study. Am J Clin Nutr 106:1032-1040.

Reddi S, Thakker-Varia S, Alder J, Giarratana AO (2022) Status of precision medicine approaches to traumatic brain injury. Neural Regen Res 17:2166-2171.

Richard NM, O'Connor C, Dey A, Robertson IH, Levine B (2018) External modulation of the sustained attention network in traumatic brain injury. Neuropsychology 32:541-553.

Røe C, Sveen U, Alvsåker K, Bautz-Holter E (2009) Post-concussion symptoms after mild traumatic brain injury: influence of demographic factors and injury severity in a 1-year cohort study. Disabil Rehabil 31:1235-1243.

Roine T, Mohammadian M, Hirvonen J, Kurki T, Posti JP, Takala RSK, Newcombe VF, Tallus J, Katila AJ, Maanpää HR, Frantzen J, Menon D, Tenovuo O (2022) Structural brain connectivity correlates with outcome in mild traumatic brain injury. J Neurotrauma 39:336-347.

Rubinov M, Sporns O (2010) Complex network measures of brain connectivity: uses and interpretations. Neuroimage 52:1059-1069.

Sánchez-Cubillo I, Periáñez JA, Adrover-Roig D, Rodríguez-Sánchez JM, Ríos-Lago M, Tirapu J, Barceló F (2009) Construct validity of the Trail Making Test: role of task-switching, working memory, inhibition/interference control, and visuomotor abilities. J Int Neuropsychol Soc 15:438-450.

Sharp DJ, Beckmann CF, Greenwood R, Kinnunen KM, Bonnelle V, De Boissezon X, Powell JH, Counsell SJ, Patel MC, Leech R (2011) Default mode network functional and structural connectivity after traumatic brain injury. Brain 134:2233-2247.

Taylor CA, Bell JM, Breiding MJ, Xu L (2017) Traumatic brain injury-related emergency department visits, hospitalizations, and deaths- United States, 2007 and 2013. MMWR Surveill Summ 66:1-16.

van den Heuvel MP, Mandl RC, Kahn RS, Hulshoff Pol HE (2009) Functionally linked resting-state networks reflect the underlying structural connectivity architecture of the human brain. Hum Brain Mapp 30:3127-3141.

van der Horn HJ, Kok JG, de Koning ME, Scheenen ME, Leemans A, Spikman JM, van der Naalt J (2017) Altered wiring of the human structural connectome in adults with mild traumatic brain injury. J Neurotrauma 34:1035-1044.

von Elm E, Altman DG, Egger M, Pocock SJ, Gøtzsche PC, Vandenbroucke JP, STROBE Initiative (2007) The Strengthening the Reporting of Observational Studies in Epidemiology (STROBE) statement: guidelines for reporting observational studies. PLoS Med 4:e296.

Wang J, Wang X, Xia M, Liao X, Evans A, He Y (2015) GRETNA: a graph theoretical network analysis toolbox for imaging connectomics. Front Hum Neurosci 9:386.

Wechsler D (1997) Wais-iii administration and scoring manual: wechsler adult intelligence scale. San Antonio, TX: Psychological Corporation.

Xia M, Wang J, He Y (2013) BrainNet Viewer: a network visualization tool for human brain connectomics. PLoS One 8:e68910.

Yeo BT, Krienen FM, Sepulcre J, Sabuncu MR, Lashkari D, Hollinshead M, Roffman JL, Smoller JW, Zöllei L, Polimeni JR, Fischl B, Liu H, Buckner RL (2011) The organization of the human cerebral cortex estimated by intrinsic functional connectivity. J Neurophysiol 106:1125-1165.

Yuan W, Wade SL, Babcock L (2015) Structural connectivity abnormality in children with acute mild traumatic brain injury using graph theoretical analysis. Hum Brain Mapp 36:779-792.

Yuan W, Treble-Barna A, Sohlberg MM, Harn B, Wade SL (2017) Changes in structural connectivity following a cognitive intervention in children with traumatic brain injury. Neurorehabil Neural Repair 31:190-201.